Molecular BioSystems

Accepted Manuscript

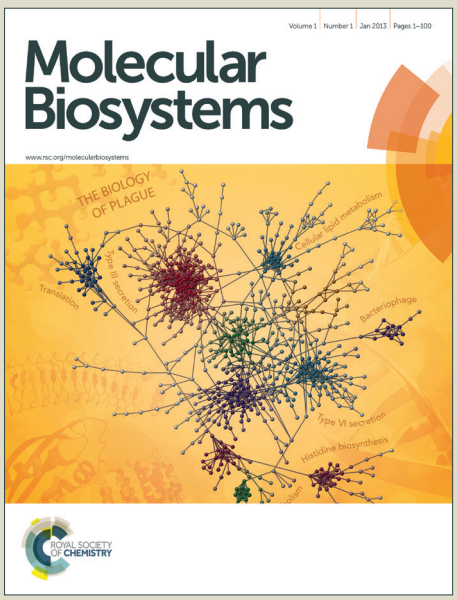

ROYAL SOCIETY OF CHEMISTRY

www.rsc.org/molecularbiosystems

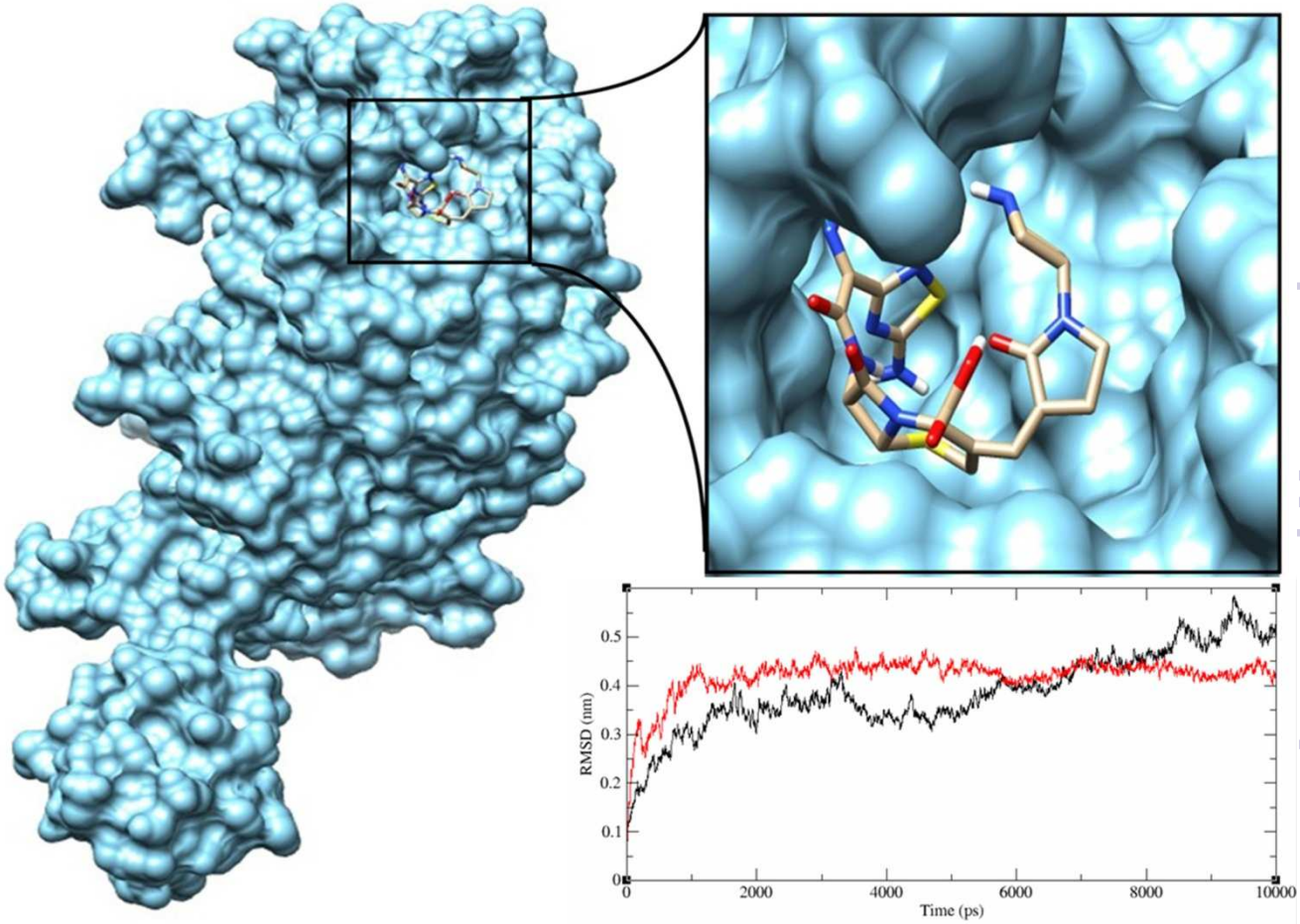

Highlights

Molecular docking analysis of β-lactam antibiotics are performed with PBP2a, PBP2b, PBP2x and SHV-1 proteins, and the best interaction is observed between Ceftobiprole and PBP2x complex, further the stability of complex is confirmed using simulation studies, our results shows that Ceftobiprole-PBP2x complex shows high stability as evident by RMSD, Rg and H-bonds.

Molecular docking and Molecular dynamics studies on β-lactamases and Penicillin binding proteins

K.M.Kumar, Anand Anbarasu, Sudha Ramaiah*
School of Biosciences and Technology.
VIT University, Vellore – 632014, Tamil Nadu, India.

*Corresponding authour:

Dr.Sudha Ramaiah
Sr. Asst. Professor,
VIT University,
Tamil Nadu, India.
Email: sudhaanand@vit.ac.in
Tel: +91-416-2202556. Fax: +91-416-2243092.

Abstract

Bacterial resistance to β-lactam antibiotics pose a serious threat to human health. Penicillin binding proteins (PBPs) and β-lactamases are involved in both antibacterial activity and mediation of β-lactam antibiotic resistance. The two major reasons for resistance to β-lactams include: (i) pathogenic bacteria expressing drug insensitive PBPs rendering β-lactam antibiotics ineffective and (ii) production of β-lactamases along with alteration of their specificities. Thus, there is an urgent need to develop newer β-lactams to overcome the challenge of bacterial resistance. Therefore the present study aims to identify the binding affinity of β-lactam antibiotics with different types of PBPs and β-lactamases. In this study, Cephalosporins and Carbapenems are docked in to PBP2a of *Staphylococcus aureus*, PBP2b and PBP2x of *Streptococcus pneumoniae* and SHV-1β-lactamase of *Escherichia coli*. The results reveal that Ceftobiprole can efficiently bind to PBP2a, PBP2b and PBP2x and not strongly with SHV-1 β-lactamase. Furthermore, molecular dynamics (MD) simulations are performed to refine the binding mode of docked complex structure and to observe the differences in the stability of free PBP2x and Ceftobiprole bound PBP2x. MD simulation supports greater stability of Ceftobiprole-PBP2x complex compared to free PBP2x. This work demonstrates that potential β-lactam antibiotics can efficiently bind to different types of PBPs for circumventing β-lactam resistance and opens avenues for the development of newer antibiotics that can target bacterial pathogens.

Introduction

β-lactams (Penicillins, Cephalosporins and Carbapenems) are potent inhibitors and have been used effectively over several decades against different types of bacterial infections, due to their higher effectiveness, low cost, ease of use, and minimal side effects.[1,2] β-lactam antibiotics form stable acyl enzyme complex with penicillin binding proteins (PBPs) in the bacterial cell membrane, thus inhibiting the final stages of peptidoglycan biosynthesis.[3-5] However, Gram-negative bacteria have developed resistance to β-lactams through three different strategies: (i) structural modification in PBP targets, (ii) production of β-lactamase[6-8] and (iii) active expulsion of β-lactam antibiotics via efflux pumps.[9] Penicillin binding proteins (PBPs) are enzymes that catalyze the steps involved in bacterial cell wall biosynthesis and are the target enzymes of β-lactam antibiotics.[10,11] PBPs have been classified into two types, high molecular weight (hmv) PBPs act as transpeptidases and low molecular weight (lmv) PBPs generally act as D-alanyl-D-alanine-carboxypeptidases (DD-carboxypeptidases).[12] The β-lactam antibiotics inhibit both transpeptidase and DD-carboxypeptidase activities by acylating the active-site serine of PBPs.[13] Alterations of the PBPs reduce their binding affinity for β-lactam antibiotics, resulting in drug resistance. The another common mechanism of bacterial resistance to the β-lactam antibiotics is the production of β-lactamase that inactivates β-lactams by hydrolyzing the amide group of the β-lactam ring.[14,15] Therefore there is an urgent need to tackle this bacterial resistance with the help of a newer antibiotics.

Cephalosporins have a broad spectrum of activity against Gram negative and Gram positive organisms such as *Streptococcus pneumoniae, Haemophilus influenzae, Streptococcus pyogenes, Klebsiella pneumoniae* and *Staphylococcus aureus*.[16-21] *S. aureus* and *S. pneumoniae* are leading causes of hospital and community acquired bacterial infection and they are global health threat.[22,23] However, many community based infections are becoming more difficult to treat owing to the emergence of resistant organism such as multidrug-resistant *S. pneumoniae* (MDRSP) and *methicillin-resistant S. aureus* (MRSA).[24,25] These two organisms are developing resistance to many of the β-lactam antibiotics.[26,27] *S. pneumoniae* contains six PBPs, PBP1a, PBP1b, PBP2a, PBP2b, PBP2x and PBP3. β-lactam antibiotics resistance in *S. pneumoniae* is caused by alterations in the penicillin-binding domains of one or more of these six PBPs.[28-30] Altered PBP1a, PBP2b and PBP2x are the most important PBPs for β-lactam antibiotic resistance.[29, 31-33] MRSA acquires resistance to such antibiotics due to altered PBP2a that have

low affinity for β-lactam antibiotics.[34] Several studies revealed the mechanism of resistance of *S. pneumoniae* and MRSA to β-lactams using only a few cephaloporins and Carbapenems.[35-41] This prompted us to investigate in detail using a wide spectrum of β-lactam antibiotics (both Cephalosporins and carbpenems). Our study mainly focused on PBP2a of MRSA and PBP2b, PBP2x from *S. pneumoniae*. Molecular docking studies are performed to investigate possible binding mechanism of Cephalosporins and Carbapenems with PBP2a of MRSA and PBP2b, PBP2x from *S. pneumoniae*. Furthermore, molecular dynamics (MD) simulations are carried out to refine the binding conformation of docked complex structure and to investigate the structural stability PBP2x in the absence and presence of ligand. The present study also compares Cephalospoirns and Carbapenem to find out which one exhibits the lowest binding affinity with SHV-1 β-lactamase.

Materials and Methods

Data set

Three PBPs (PBP2a, PBP2b and PBP2x) and class A type β-lactamase (SHV-1) were selected for this study. 3-Dimensional (3D) structures of the PBPs and β-lactamase were obtained from Protein Data Bank (PDB).[42] Co-crystallized ligands were identified and removed from the target proteins and then crystallographic water molecules were eliminated from the 3D coordinate file. Missing side chains were reconstructed to the target protein structures and minimizations were performed using SwissPDBviewer.[43] The structues of β-lactam antibiotics were obtained from NCBI PubChem Compound database[44] and the structures were drawn using Chemsketch.[45] Hydrogen atoms were added to all the structures and gasteiger atomic partial charges were computed. A geometry optimization of all the compounds was performed by using chimera[46] for flexible conformations of the compounds during the docking. The PDB ID, source and detail of PDB structures employed for the study are listed in Table 1.

Molecular docking using Surflex2.0

Molecular docking analysis was carried out to identify the variations in the binding affinity of β-lactam antibiotics with PBPs (PBP2a, PBP2b and PBP2x) and SHV-1 β-lactamases. The target protein was imported into SYBYL molecular graphical interface. Using the biopolymer structure preparation module available in SYBYL2.0[47], charges were assigned according to AMBER FF99

force field, hydrogens were added and missing side chains were fixed to the target protein. Ligand molecules were then optimized using Tripos force field. Hydrogen atoms were added and the structures were subjected for energy minimization using tripos force field. The Surflex-Dock algorithm in SYBYL 2.0[48] was used for molecular docking calculation. The algorithm generated ideal ligand binding site called "protomol", as a target to generate possible ligand binding pose for β-lactam antibiotics. These possible ligand binding poses were scored using the Hammerhead scoring function.[49,50] The scoring function contains the polar contact terms, hydrophobic and solvation terms. In this study the differences in binding affinity of β-lactam antibiotics with PBPs and SHV-1 β-lactamase was analyzed. The docking scores were generated in -logKd units to represent the calculated-binding affinities. The maximum number of poses per ligand was set to 10. No constraints were assigned for this procedure. The docking complex was validated using total score (dock score), further 3D structures of PBPs were analysed and visualized through PyMOL viewer.[51] Hydrophobic contacts are analyzed using Ligplot.[52] Solvent accessible surface areas were analysed for Target protein using Get area online server.[53]

Molecular dynamics simulation

The simulation of the enzyme in the presence and absence of ligand was performed using the GROMACS 4.5.5 software.[54] Ceftobiprole has least docking score when compared to other compounds. MD simulation was carried out for PBP2x-Ceftobiprole docked complex. The topology of the enzyme was created using GROMACS utilities, where as the topology of the ligand was generated using the PRODRG server[55] in the framework of the force field GROMOS96 43a1.[56,57] All starting structures were solvated in a simple point charge[68] water box under periodic boundary conditions using 1.0 nm distance from the protein to the box faces. Each system was then neutralized by Cl^- or Na^+ counter ions (PBP2x and PBP2x-Ceftobiprole system respectively). Following steepest descents energy minimization, the systems were equilibrated under NVT (constant number of particles, volume and temperature) conditions for 100 ps at 300K, followed by 100 ps under NPT (constant number of particles, pressure, and temperature) conditions. All the covalent bonds were constrained using the LINCS (Linear Constraint Solver) algorithm.[59] The electrostatic interactions were treated using the Particle Mesh Ewald (PME) method.[60] The cutoff radii for coulomb and van der Waals interactions were

set to 10.0 and 14.0 Å, respectively. Finally, 10ns MD was performed in order to analyse the stability of each system.

The potential of each trajectory produced after MD simulations were analysed. The MD trajectories were analysed using g_rms, g_rmsf, g_hbond and g_gyrate of GROMACS utilities[61] to obtain the root-mean-square deviation (RMSD), root-mean-square fluctuation (RMSF), radius of gyration (Rg) and the number of H-bond formed between the ligand and proteins. The differences in the kinetic, potential and total energies, pressure and temperature were computed as a function of simulation time to check whether the systems obey NVT or NPT ensemble throughout the simulation. The number of hydrogen bonds was calculated to understand the difference in ligand-protein stability. The trajectories were analyzed using the tools from GROMACS distribution. All the graphs were generated using XMgrace tool.[62]

Essential dynamics (ED)

Essential dynamics (ED)[63,64] was performed for all the trajectories. The GROMACS inbuilt tools g_covar & g_anaeig were used for performing ED analysis. The trajectory file of a MD simulation was utilized to identify the dominant motions of the PBP2x in the presence and absence of Ceftobiprole. The first two eigenvectors (principal components PC1 and PC2) with largest eigenvalues were used to make 2D projection for each of independent trajectories. ED analysis was applied to extract the principal modes involved in the motion of the protein molecule.

Results and discussion

Ligand conformation

Evaluation of binding affinity of β-lactam antibiotics with PBP2a, PBP2b, PBP2x and SHV-1 β-lactamase are performed using Surflex dock. The binding poses for each ligand molecule into the PBPs and SHV-1 β-lactamase are determined and different poses are generated based on the total score (Dock score). The total score is an indicator of the binding affinity of a ligand-receptor complex. The docking scores ($-\log K_d$) for fourth and fifth generation Cephalosporins and Carbapenems are depicted in Table 2. The binding conformation for each ligand molecule into the PBP2a, PBP2b, PBP2x and SHV-1 β-lactamase target proteins are determined and the one having highest docking score with PBPs and lower docking score with SHV-1 β-lactamase are

generated. The higher docking scores represent better protein-ligand binding affinity compared to lower docking score values. Among the 13 ligands, the fifth generation cephalosporin, Ceftobiprole has high docking score value with PBPs (Dock score for PBP2a=5.2, PBP2b=5.6, PBP2x=6.0) and low docking score for SHV-1 β-lactamase (Dock score SHV-1=3.2). From the docking results, the variation is observed in the binding affinity of Ceftobiprole with PBP2a, PBP2b, PBP2x and SHV-1 β-lactamase. Ceftobiprole shows high binding affinity with PBPs especially it has highest binding affinity with PBP2x where as for SHV-1 β-lactamase binding affinity of Ceftobiprole is lower. We further analyzed the docked conformation for finding the binding mode of Ceftobiprole into PBP2a, PBP2b, PBP2x and SHV-1 β-lactamase target proteins to validate the position obtained likely to represent reasonable binding conformations.

Docking of Ceftobiprole into Penicillin binding proteins (PBP2a, PBP2b and PBP2x)

Binding affinity of Ceftobiprole towards PBP2a, PBP2b and PBP2x are investigated in detail. The number of H-bonds and binding residues of PBP2a, PBP2b and PBP2x with Ceftobiprole complexes are shown in Table 3-6. From the post docking analysis, it is found that the Ceftobiprole shows high binding affinity with PBP2a, PBP2b and PBP2x. On analysis of the interaction of Ceftobiprole in the active site of PBP2a, PBP2b and PBP2x, it is observed the residues Gln292, Asp295 and His293 in PBP2a are participating in the H-bond interaction (Fig. 1A). From the Fig 1A, it is found that His293 and Asp295 contributed more number of H-bond interaction with Ceftobiprole. Moreover these two residues are present in buried region of protein structure. In PBP2b, Lys241, Arg223, Ser239, Glu240, Ser238 and Arg262 residues are in H-bond contact with Ceftobiprole (Fig. 1B). Hydroxyl (Ser 239) and Polar residues (Arg223 and Arg262) are very crucial in hydrogen bond formation between Ceftobiprole and PBP2b and they formed 5 hydrogen bonds with Ceftobiprole. Among these residues, Arg223, Glu240 and Ser238 are located in buried region of PBP2b structure. In PBP2x, the amino acid residues Asp313, Asp90, Ala91, Thr92 and Ser93 are shown H-bond interaction with Ceftobiprole (Fig. 1C). The interaction analysis of Ceftobiprole-PBP2x complex reveals that hydroxyl amino acids (Thr92 and Ser93) and acidic amino acids (Asp313 and Asp90) have crucial role in the formation of hydrogen bond with Ceftobiprole and they contributed 7 hydrogen bonds (Table.7).

Docking of Ceftobiprole in to SHV-1 β-lactamase

Docking analysis of β-lactam antibiotics with SHV-1 β-lactamase is carried out to identify the drug which is having lowest binding affinity with SHV-1 β-lactamase. Among the 13 β-lactam antibiotics selected for this study, Ceftobiprole shows the dock score value of 3.2 (Table. 2). It is lower when compared to other β-lactam antibiotics. It indicates Ceftobiprole has lower binding affinity with SHV-1 β-lactamase. From the interaction residues analysis, it is observed that only three amino acid residues Arg276, Gln270 and Asn132 are involved in the interaction with Ceftobiprole and formed less number of hydrogen bonds (Table 6). Among these interacting residues, Asn132 is present in buried region of protein structure. The possible binding mode of Ceftobiprole into the binding site of SHV-1 β-lactamase and corresponding 2D interaction models, number of hydrogen bonds and bond distance are shown in Table 7 and Fig 1D.

Hydrophobic interaction

Hydrophobic interactions are also a crucial element of binding for Ceftobiprole. Hydrophobic interactions should play an important role in the ligand-protein interaction. The residues of PBPs (PBP2a, PBP2b and PBP2x) and SHV-1 β-lactamase involved in the hydrophobic interaction with Ceftobiprole are analysed using Ligplot tool (Fig. 2). In PBP2a, Tyr297, Asn146, Lys273, Asp295, Glu294 and Val277 are in hydrophobic contact with Ceftobiprole (Fig. 2A). From the interaction residues analysis, it is observed the residues Lys241, Asp222, Ser238 and Val237 of PBP2b are involved in hydrophobic interaction with Ceftobiprole (Fig. 2B), Among these residues Ser238 and Val237 are present in buried region of protein structure, Hence these two residues are very crucial in hydrophobic contact with Ceftobiprole. On analysis of the interaction of Ceftobiprole in the active site of PBP2x, it is observed the seven residues Asn 185, Ser187, Ala91, Thr159, Glu89, Ser93 and Thr92 are participating in hydrophobic interaction (Fig. 2C). In SHV-1 β-lactamase, only four residues Tyr241, Asp240, Gly238 and Tyr105 are hydrophobic contact with Ceftobiprole (Fig. 2D). These observations are significant and might be the probable cause for higher affinity of Ceftobiprole to PBPs and lower binding affinity to SHV-1 β-lactamase.

Molecular dynamics simulation

MD simulations are conducted for the protein-ligand complex as well as for the free enzyme. This provided a better picture of the overall stability of the PBP2x and PBP2x complex with Ceftobiprole within nanosecond time scale. Ceftobiprole-PBP2x complex is selected because Ceftobiprole has high binding affinity with PBP2x. The complex model and the free enzyme are subjected to 10 ns MD simulations in order to find the stability of the PBP2x in the presence of the Ceftobiprole. Root-mean-square-deviation (RMSD), Root mean square fluctuation (RMSF), Radius of gyration (Rg) and H-bonds are used to check the stability of the model system.

Root mean square deviation

The RMSD, a crucial parameter to analyse the equilibration of MD trajectories. RMSD of the protein backbone atoms are plotted as a function of time to check the stability of the each system throughout the simulation. The RMSD values of the PBP2x backbone with and without Ceftobiprole are calculated against the simulation time scale (0-10000 ps) and results are shown in Fig 3. It can be noted that two trajectories have RMSD values within 0.1- 0.6 Å during 10000 ps simulation. From the Fig 3, it is seen that for free PBP2x system, The RMSD values is 0.35 nm at 6000 ps. After this, the RMSD value is increased up to 0.6 nm. For PBP2x-Ceftobiprole complex, the RMSD values steadily increase till 3000 ps followed by a slow increase up to 4500 ps. After this there is no further increment of RMSD values and the complex systems reached equilibrium. After 6000 ps, PBP2x-Ceftobiprole complex system shows lower RMSD value than the free PBP2x system. The decrease in RMSD value of the complex from that of the free PBP2x indicates increased rigidity and stability of the PBP2x upon binding with Ceftobiprole.

Root mean square fluctuation

The RMSF with respect to the average MD simulation conformation is used as a mean describing flexibility differences among residues. The RMSF of the backbone atoms of each residue in the PBP2x-Ceftobiprole and in free PBP2x is calculated to reveal the flexibility of the backbone structure. The high RMSF value shows more flexible where as low RMSF value shows limited movements during simulation in relation to its average position. The RMSF of the residues are shown in Fig 4, clearly depicting different flexibility in the PBP2x in the absence and presence of Ceftobiprole. In Fig 4, it is found that the residues (100-156 and 558-566) in

PBP2x without Ceftobiprole show more fluctuation than the PBP2x-Ceftobiprole complex. The residues in the PBP2x that bind with the Ceftobiprole shows a small degree of flexibility with RMSF of less than 4.00 nm when compared with the free PBP2x, reveals that the residues of PBP2x in the presence of Ceftobiprole seem to be more rigid as a result of binding to Ceftobiprole.

Radius of gyration and H-bond network

We also performed Rg to understand the level of compaction in the structure of PBP2x in the absence and presence of Ceftobiprole. The Rg is defined as the mass weighted root mean square distance of a collection of atoms from their common center of mass. Hence this analysis gives us the overall dimensions of the protein. The calculated Rg values over the simulation time scale for the PBP2x and the PBP2x-Ceftobiprole complex are shown in Fig 5. Rg value of PBP2x-Ceftobiprole and free PBP2x varies between 2.55 nm to 2.75 nm. As shown in Fig 5, it is observed that for PBP2x, the Rg values fluctuate near 2.76 nm and then decrease to a minimum value of 2.68 nm and for PBP2x-Ceftobiprole complex the Rg value initially fluctuate near 2.60 nm after 200 ps the Rg value is decreased up to 2.50 nm. From the Rg plot, it is clear that the PBP2x and PBP2x-Ceftobiprole complex curve differs significantly and PBP2x-Ceftobiprole complex shows lower Rg value than the PBP2x. During simulation the change of Rg value from PBP2x to PBP2x-Ceftobiprole over simulation time reveals stabilization and little conformational changes in PBP2x when bound to the Ceftobiprole. The intermolecular hydrogen bonding between the protein and ligand plays an essential role in stabilizing the protein-ligand complexes. The stability of hydrogen bond network formed between Ceftobiprole and PBP2x is calculated throughout the simulation for the ligated system. Total number of H-bonds in Ceftobiprole-PBP2x complex versus time at 300K is shown in Fig 6. Ceftobiprole-PBP2x complex exhibited seven H-bonds throughout the simulation time period. It indicates that the Ceftobiprole shows stable and strong H-bonds with PBP2x.

Essential dynamics analysis

The confined fluctuation and structural motion of the PBP2x in the absence and presence of Ceftobiprole are determined using ED analysis. The molecular dynamics snapshots at every 2ps are projected on to the first two eigenvectors, the two most principal components out of 25 are calculated. The spectrum of the corresponding eigenvalues represents that the structural motion

of the system is basically confined within the first two eigenvectors. The projections of trajectories obtained at 300 K on to the first two principal components (PC1 and PC2) showed the structure motion of PBP2x and PBP2x-Ceftobiprole complex in phase space. The 2D plots of two principal components (PC1 and PC2 with largest eigenvalues) for PBP2x and PBP2x-Ceftobiprole complex are depicted in Fig 7. More distribution of dots indicates the more conformational changes in protein structure. From the Fig 7, it clearly depicts that the distribution for free form of PBP2x is large compared to the Ceftobiprole bound form. The internal motions of PBP2x-Ceftobiprole represented by a subspace whose dimension is much smaller than the PBP2x. It is obviously due to the rigidity introduced by binding of Ceftobiprole.

Conclusion

In the present study, the molecular docking and MD simulations are performed to investigate the reasonable binding conformation of β-lactam antibiotics with PBP2a of *S. aureus,* PBP2b and PBP2x *of S. pneumoniae*. The best docked conformation is selected based on binding energy scores, hydrogen bonding and hydrophobic interaction. Cephalosporins show higher affinity with PBPs than Carbapenems. Especially the fifth generation Cephalosporin, Ceftobiprole shows best results with PBP2a, PBP2b and PBP2x. The conclusion drawn from this docking is that Ceftobiprole has the highest binding affinity with PBP2x of *S. pneumoniae.* Several Class-A β-lactamase enzymes have the potential to hydrolyze Cephalosporins. Therefore, the present study also investigated the binding affinity of β-lactams (Cehaplospoirns and Carbapenems) with SHV-1 β-lactamase and solvent accessible surface area of amino acid residues involved in both H-bond and hydrophobic interactions with Ceftobiprole are identified. Our observations on amino acid residues in the active site suggest, that they are buried in PBPs and there are more hydrophobic and H-bond interactions with Ceftobiprole. However, the residues in the active site of SHV-1 β-lactamase are exposed and there are only a few H-bond and hydrophobic interactions with Ceftobiprole. Thus Ceftobiprole may not be hydrolyzed by SHV-1 β-lactamase while it binds strongly to PBPs. Furthermore, MD simulation is performed to check the stability of the Ceftobiprole-PBP2x complex. RMSD, RMSF, Rg, H-bond and PCA results indicates that Ceftobiprole-PBP2x complex is highly stable compared to free PBP2x. Over all, from the results of the present study, it is strongly suggested that Ceftobiprole is a potent inhibitor of PBP2a,

PBP2b and PBP2x which can be further modified and explored as a potential next generation β-lactam antibiotic for *S. aureus* and *S. pneumoniae* infections.

Abbreviations

PBP - Penicillin binding protein
MRSA - *Methicillin-resistant S. aureus*
MDRSP- *Multidrug-resistant S. pneumoniae*
PDB - Protein data bank
ADT - AutoDockTools
MD - Molecular dynamics
ED - Essential dynamics
RMSD - Root mean square deviation
RMSF - Root mean square fluctuation
Rg - Radius of gyration
PC - Principal component
H-bond- Hydrogen bond
SPC - Simple point charge
NPT - Constant Number of particles, pressure and temperature
NVT - Constant Number of particles, volume and temperature
LINCS - Linear Constraint Solver
PME - Particle mesh Ewald

Acknowledgement

Dr. Anand Anbarasu gratefully acknowledges the Indian council of Medical Research (ICMR), Government of India Agency for the research grant [IRIS ID:2011-03260]. The authors would also like to thank the management of VIT University for providing the necessary facilities to carry out this research project.

References:

1. J. M. Frere, and B. Joris, *Critical Reviews in Microbiology*, 1985, 11, 299-396.
2. A. Matagne, A. Dubu, M. Galleni and J. M Frere, *Natural product reports,* 1999, 16(1), 1-19.
3. P. Macheboeuf, C. Contreras-Martel, V. Job, O. Dideberg and A. Dessen, *FEMS Microbiol. Rev*., 2006, 30, 673-691.
4. E. Chain, *Annual review of Biochemistry,* 1948b, 17*,* 657-704.
5. H. Florey, *Advancement of Science,* 1948, 4, 281-6.

6. J. D. Williams and F. Moosdeen, *Rev. Infect. Dis*., 1986, 8(5), S555-61.

7. A. J. Reid, I. N. Simpson, P. B. Harper and S. G. Amyes, *J. Antimicrob Chemother*., 1987, 20, 645-656.

8. J. H. Jorgensen, *Clin. Infect. Dis*., 1992, 14, 1119-1123.

9. M. S. Wilke, A. L. Lovering and N. Y. C. Strynadka, *Curr. Opin. Microbio.,* 1948, l8, 525-533.

10. J. F. Fisher, S. O. Meroueh, and S. Mobashery, *Chem. Rev*., 2005, 105, 395-424.

11. P. Macheboeuf, C. Contreras-Martel, V. Job, O. Dideberg, and A. Dessen, *FEMS Microbiol. Rev.,* 2006, 30, 673-691.

12. M. A. McDonough, J. W. Anderson, N. R. Silvaggi, R. F. Pratt, J. R. Knox, and J. A. Kelly, *J. Mol. Biol*., 2002, 322, 111-122.

13. R. Hakenbeck, *Electrophoresis*, 1998, 19, 597-601.

14. A. Matagne, B. A. Misselyn, B. Joris, T. Erpicum, B. Granier, and J. M. Freare, *Biochemical Journal*, 1990, 265, 131-146.

15. A. Matagne, and J. M. Freare, *Biochimica et Biophysica Acta,* 1995, 1246, 109-127.

16. C. L. Clark, K. Nagai, B. E. Dewasse, G. A. Pankuch, L. M. Ednie, M. R. Jacobs and P. C. Appelbaum, *J. Antimicrob. Chemother.,* 2002, 50, 33-41.

17. A. Fenoll, M. J. Gimenez, O. Robledo, P. Coronel, M. Gimeno, J. Casal and L. Aguilar, *Int. J. Antimicrob. Agents,* 2007, 29, 224-226.

18. M. Y. Lee, K. S. Ko, W. S. Oh, S. Park, J. Y. Lee, J. Y. Baek, J. Y. Suh, K. R. Peck, N. Y. Lee and J. H. Song, *Int. J. Antimicrob. Agents*, 2006, 28, 14-18.

19. A. Shimizu, K. Maebashi, M. Niida, T. Mikuniya, M. Hikida, and K. Ubukata, 2007, *J. Korean Med. Sci*., 22, 20-25.

20. F. Soriano, J. J. Granizo, A. Fenoll, M. Gracia, R. Fernandez-Roblas, J. Esteban, I. Gadea, P. Coronel, M. Gimeno, E. Rodenas and F. Santos, *J. Chemother*., 2003, 15, 107-112.

21. F. Soriano, J. J. Granizo, P. Coronel, M. Gimeno, E. Rodenas, M. Gracia, C. Garcia, R. Fernandez-Roblas, J. Esteban, and I. Gadea, *Int. J. Antimicrob. Agents*, 2004, 23, 296-299.

22. H. F. Chambers, *Clin. Microbiol. Rev*., 1997, 10, 781-791.

23. M. C. Enright, D. A. Robinson, G. Randle, E. J. Feil and H. Grundmann, *Proc. Natl. Acad. Sci. U S A*, 2002, 99, 7687-7692.

24. F. Van Bambeke, R. R. Reinert, P. C. Appelbaum, P. M. Tulkens and W. E. Peetermans, *Drugs,* 2007, 67, 2355-82.

25. C. Stankovic, P. V. Mahajan, and B. I. Asmar, *Curr. Infect. Dis. Rep.*, 2007, 9, 223-7.

26. C. H. Chiu, L. H. Su, Y. C. Huang, J. C. Lai, H. L. Chen, and T. L. Wu, *Antimicrob Agents Chemother*., 2007, 51, 3404-6.

27. N. S. Niederman, *Chest*, 2007, 131, 1205-15.

28. R. Hakenbeck, A. Konig, I. Kern, M. Van Der Linden, W. Keck, D. Billot- Klein, R. Legrand, B. Schoot and L. Gutmann, *J. Bacteriol*., 1998, 180, 1831-1840.

29. R. Hakenbeck, *Chemotherapy*, 1999, 45, 83-94.

30. G. Laible, B. G. Spratt and R. Hakenbeck, *Mol. Microbiol*., 1991, 5, 1993-2002.

31. Y. Asahi, Y. Takeuchi, and K. Ubukata, *Antimicrob. Agents Chemother*., 1999, 43, 1252-1255.

32. Y. Asahi and K. Ubukata, *Antimicrob. Agents Chemother*., 1998, 42, 2267-2273.

33. A. M. Smith, and K. P. Klugman, *Antimicrob. Agents Chemother*., 1995, 39, 859-867.

34. H. Liu, G. Buescher, N. Lewis, S. Snyder and D. Jungkind*, European Journal of Clinical Microbiology and Infectious Diseases*, 1990, 9, 717–724.

35. H. S. Sader, T. R. Fritsche and R. N. Jones, *Antimicrob. Agents Chemother.*, 2008, 52, 1153-5.

36. A.Villegas-Estrada, M. Lee and D. Hesek, *J. Am. Chem. Soc.*, 2008, 130, 9212-3.

37. H. F. Chambers and M. Sachdeva, *J. Infect. Dis., 1990*, 161, 1170-6.

38. G. Laible, B. G. Spratt and R. Hakenbeck, *Mol. Microbiol*., 1991, 5, 1993-2002.

39. L. McGee, D. Biek and Y. Gel, *Antimicrob. Agents Chemother.*, 2009, 53, 552-6.

40. F. Malouin, J. Blais and S. Chamberland, *Antimicrob. Agents Chemother.*, 2003, 47, 658-64.

41. T. A. Davies, M. G. P. Page and W. Shang, *Antimicrob. Agents Chemother.,* 2007, 51, 2621-4.

42. H. M. Berman, J. Westbrook, Z. Feng, G. Gilliland, T. N. Bhat, H. Weissig, I. N. Shindyalov, and P. E. Bourne, *Nucleic Acids Research,* 2000, 28*,* 235-242.

43. N. Guex and M. C. Peitsch, *Electrophoresis,* 1997, 18, 2714-2723.

44. Q. Li, T. Cheng, Y. Wang, and S. H. Bryant, *Drug Discov. Today,* 2010, 15, 1052-1057

45. Z. Li, H. Wan, Y. Shi, and P. Ouyang, *Journal of Chemical Information and Computer Sciences,* 2004, 44*,* 1886-90.

46. E. Pettersen, T. D. Goddard, C. C. Huang, G. S. Couch and D. M. Greenblatt, *Journal of Computational Chemistry,* 2004, *2,* 1605-1612.

47. SYBYL/Surflex-Dock, version 2.0; Tripos Inc. St. Louis, MO, 2007.

48. A. N. Jain, *Journal of Medicinal Chemistry,* 2003, 46*,* 499-511.

49. A. N. Jain, *Journal of computer-Aided Molecular Design,* 1996, 10, 427-40.

50. W. Welch, J. Ruppert, and A.N. Jain, *Chemistry & Biology,*1996*,* 3*,* 449-62.

51. M. A. Lill and M. L. Danielson, *J. Comput. Aided Mol. Des.,* 2010, *25*, 13-19.

52. A. C. Wallace, R. A. Laskowski and J. M. Thornton, *Protein Eng*., 1995, 8, 127-134.

53. R. Fraczkiewicz, W. Braun, *Journal of Computational Chemistry*, 1998, 19, 319-333.

54. B. Hess, C. Kutzner, D. Van der Spoel and E. Lindahl, *Journal of Chemical Theory and Computation,* 2008, 4*,* 435-447.

55. A. W. Schuttelkopf and D. M. van Aalten, *Section D, Biological Crystallography*, 2004, 60, 1355-1363.

56. W. F. V. Gunsteren, S. R. Billeter, A. A. Eising, P. H. Hunenberger**,** P. K. Kruger, A. E. Mark, W. R. P. Scott, and I. G. Tironi, *Verlag der Fachvereine, ZUrich,* 1996, 1-1024.

57. C. Oostenbrink, A. Villa, A. E. Mark and W. F. V. Gunsteren, *Journal of Computational Chemistry,* 2004, 25*,* 1656-1676.

58. H. J. C. Berendsen, J. P. M. Postma, W. F. V. Gunsteren and J. Hermans, *D Reidel Publishing Company Dordrecht,* 1981, 331-342.

59. B. Hess, H. B. Herman, J. C. Berendsen, G. E. M. Johannes and Fraaije, *Journal of Computational Chemistry,* 1997, 18*,* 1463-1472.

60. U. Essmann, L. Perera, M. L. Berkowitz, T. Darden, H. Lee, and L. G. Pedersen, *Journal of Chemical Physics,* 1995, 103*,* 8577-8593.

61. D.Van der Spoel, E. Lindahl, B. Hess, G. Groenhof, A. E. Mark and H. J. Berendsen, *J. Comput. Chem.,* 2005, 26, 1701-1718.

62. P. J. Turner, Center for Coastal and Land-Margin Research, Oregon Graduate Institute of Science and Technology, Beaverton, Ore, USA, 2005.

63. A. Amadei, A. B. Linssen and H. J. Berendsen, *Proteins: Struct., Funct., Genet*., 1993, 17, 412-425.

64. D. Janezic, R. M. Venable, B. R. Brooks, *Journal of Computational Chemistry*, 1995, 16, 1554-1566.

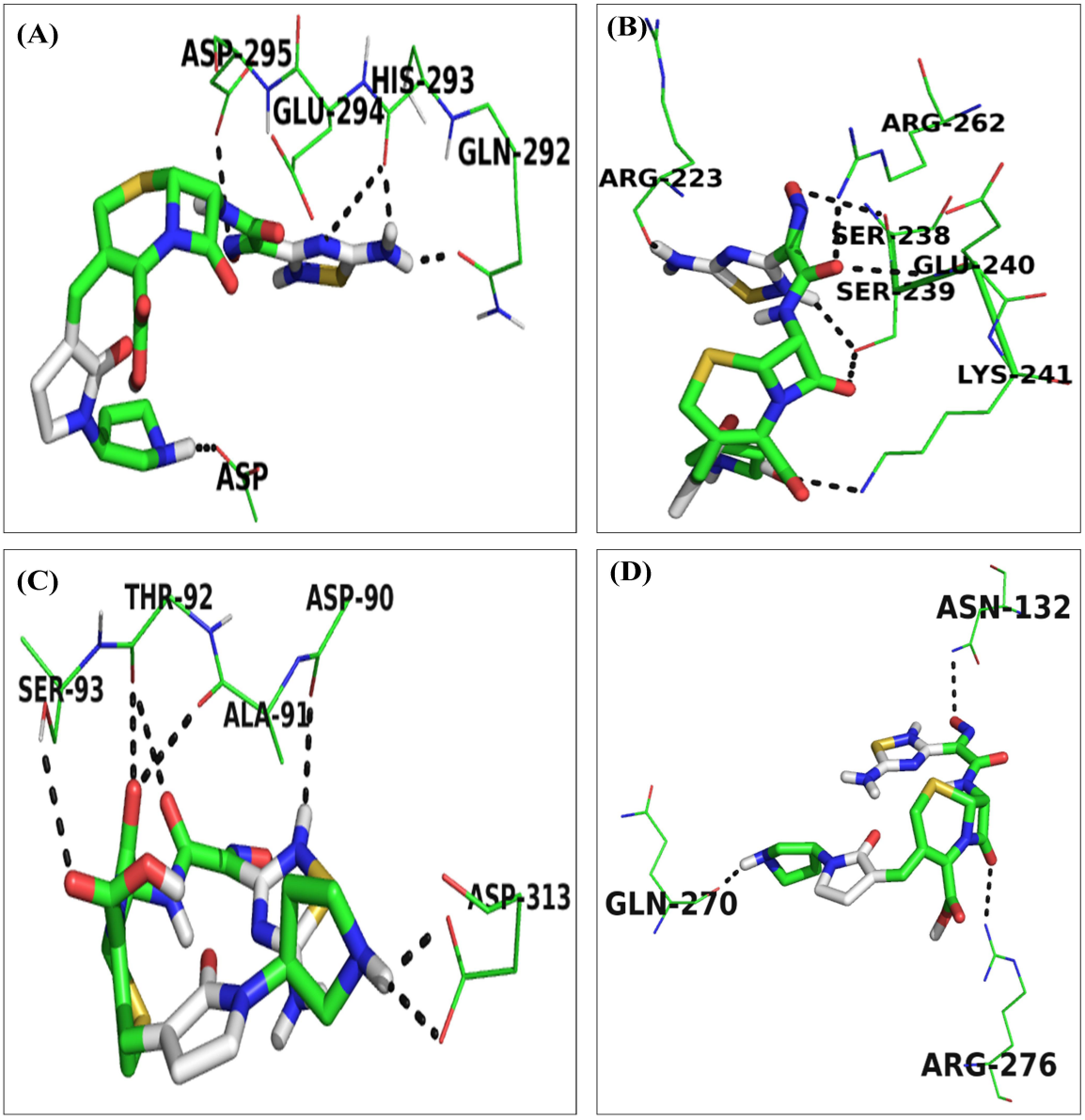

Fig. 1 Docking results of Ceftobiprole in to PBP2a, PBP2b, PBP2x and SHV-1. (A) Binding mode of Ceftobiprole in PBP2a. (B). A close-up view of the binding site of Ceftobiprole in PBP2b. (C) Ceftobiprole interaction with PBP2x. (D) Binding mode of Ceftobiprole with SHV-1. Ligand atoms are coloured by its type. The interacted amino acids residues, hydrogen bond networks in the binding pocket are all shown.

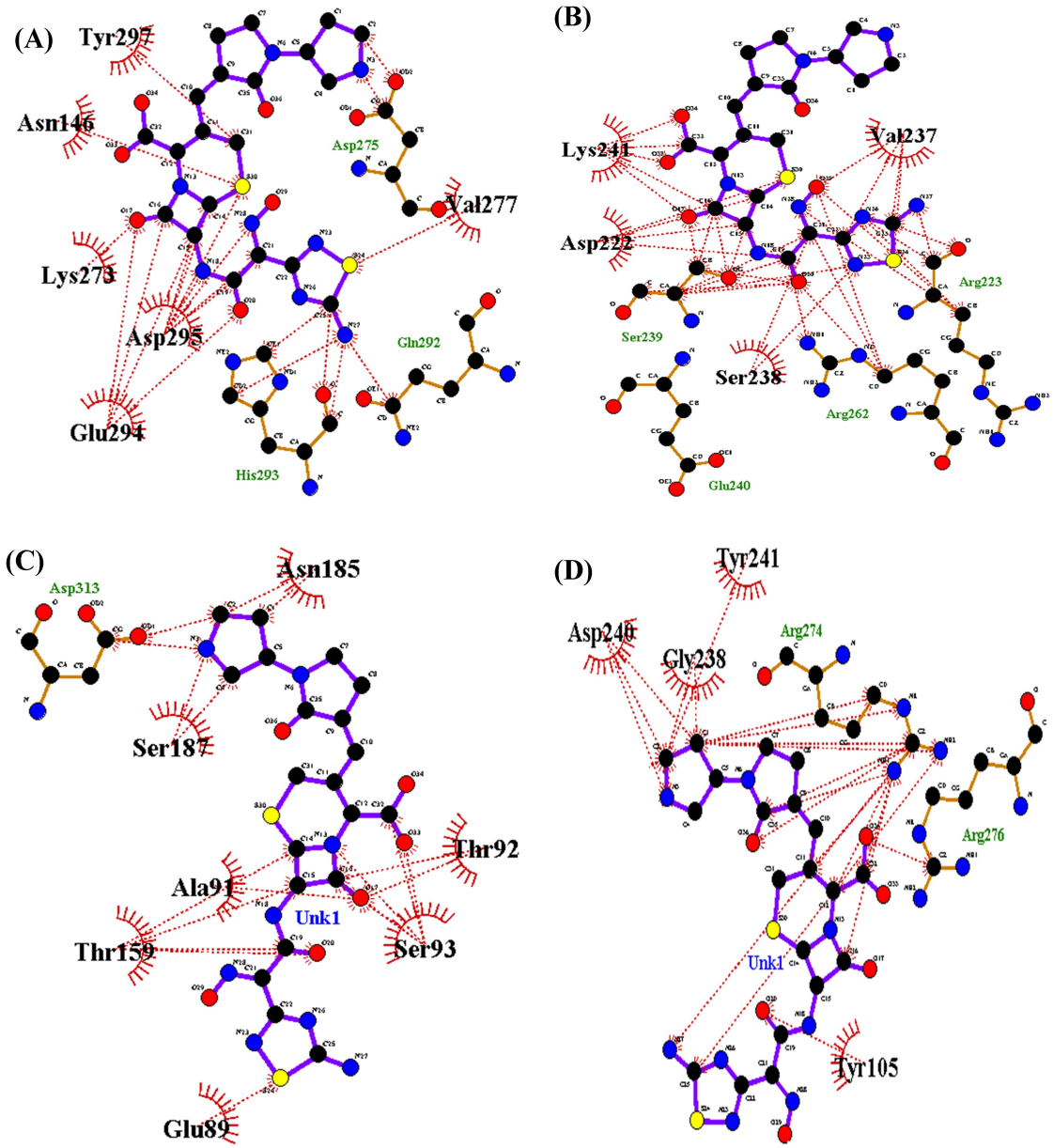

Fig. 2 Schematic representation of the hydrophobic interaction between Ceftobiprole with A) PBP2a (B) PBP2b (C) PBP2x and (D) SHV-1 produced using the LIGPLOT program [43]. Hydrophobic contacts are indicated by an arc with spokes radiating towards the ligand atoms they contact. The interacted atoms are spokes radiating back.

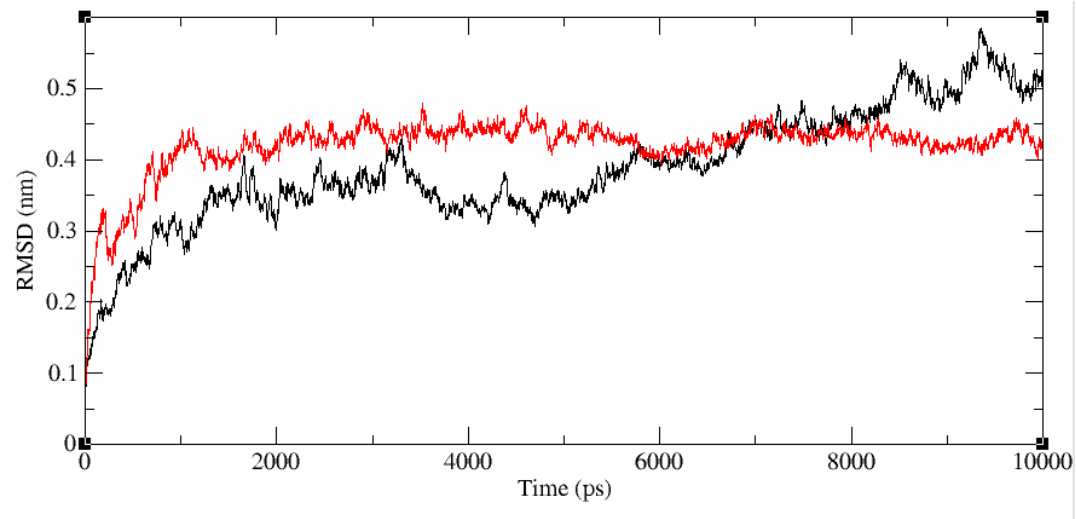

Fig. 3 Backbone RMSDs are shown for PBP2x in the absence and presence of Ceftobiprole at 300K. Black color indicates PBP2x in the absence of Ceftobiprole, PBP2x-Ceftobiprole complex shown in red.

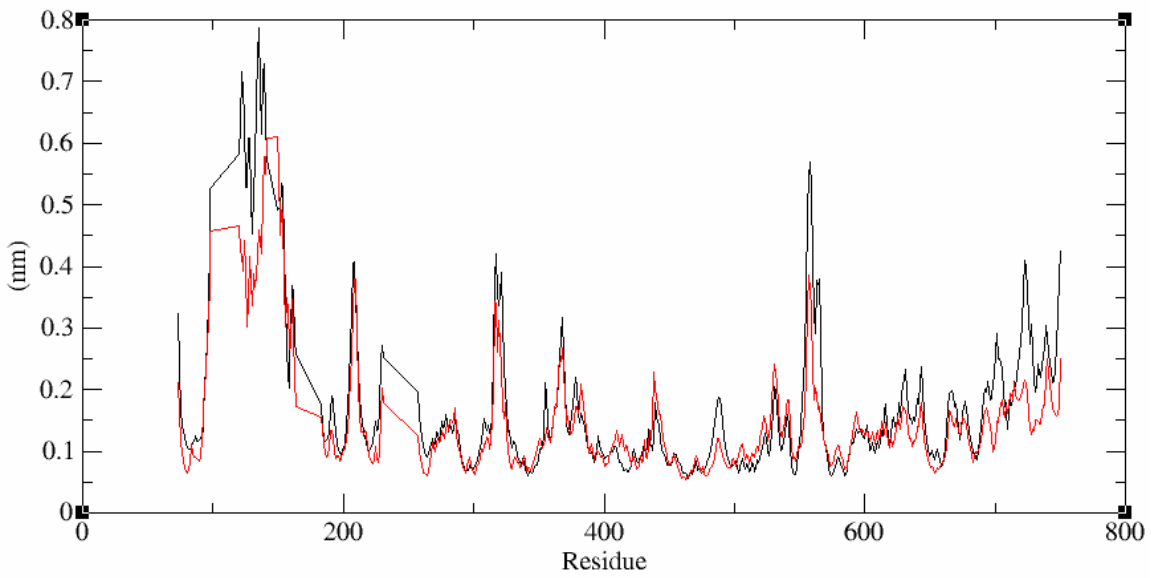

Fig. 4 RMSF of the backbone atoms of PBP2x in the presence and absence of Ceftobiprole at 300K. Black color indicates PBP2x in the absence of Ceftobiprole, PBP2x-Ceftobiprole complex shown in red.

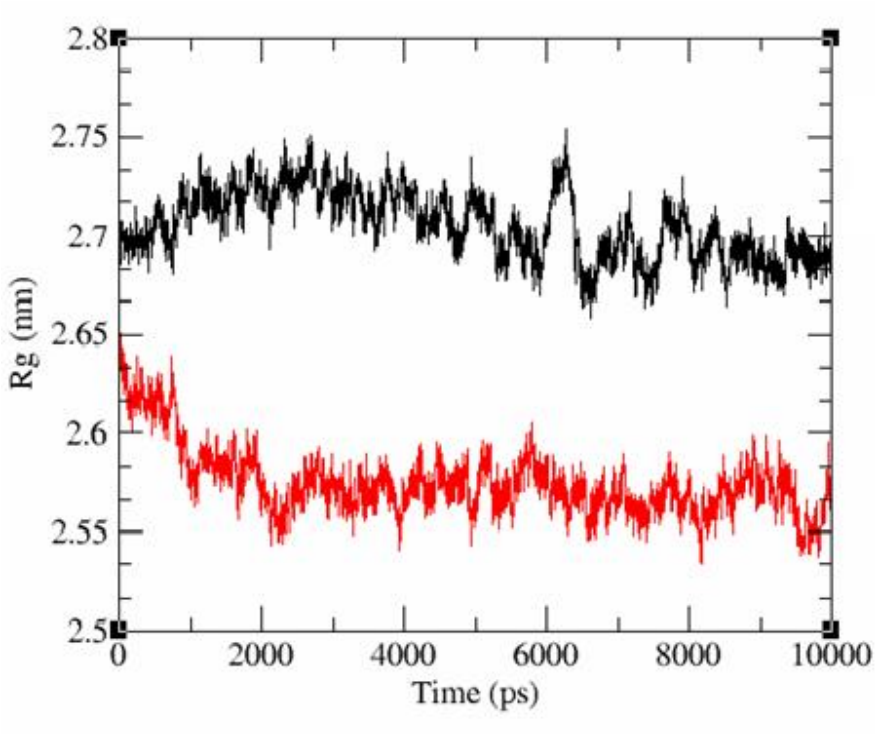

Fig. 5 Radius of gyration of Cα atoms of PBP2x in the presence and absence of Ceftobiprole. Black color indicates PBP2x in the absence of Ceftobiprole, PBP2x-Ceftobiprole complex shown in red.

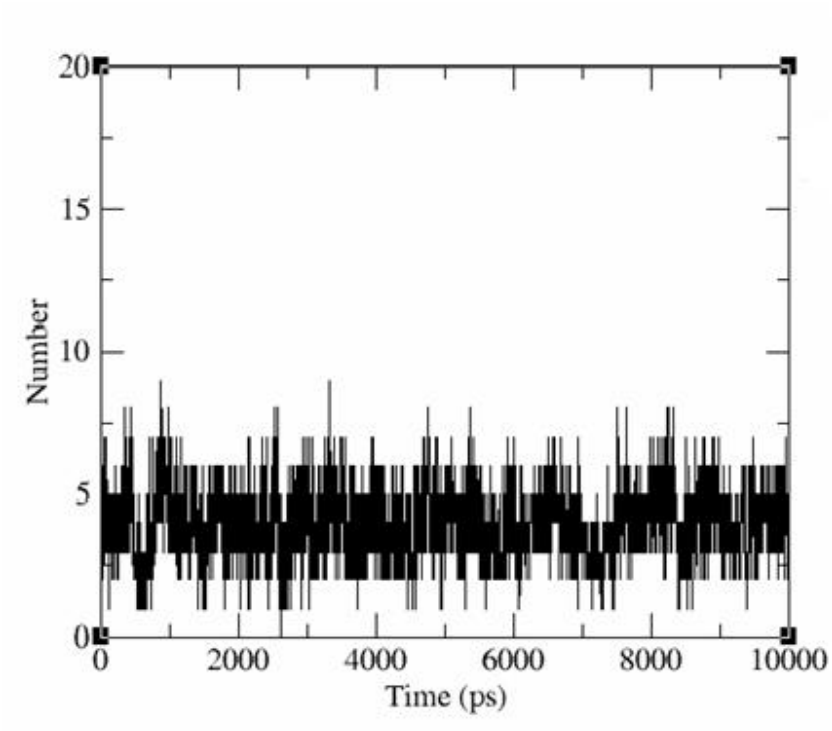

Fig. 6 Total number of H-bond between Ceftobiprole-PBP2x complex versus time at 300K.

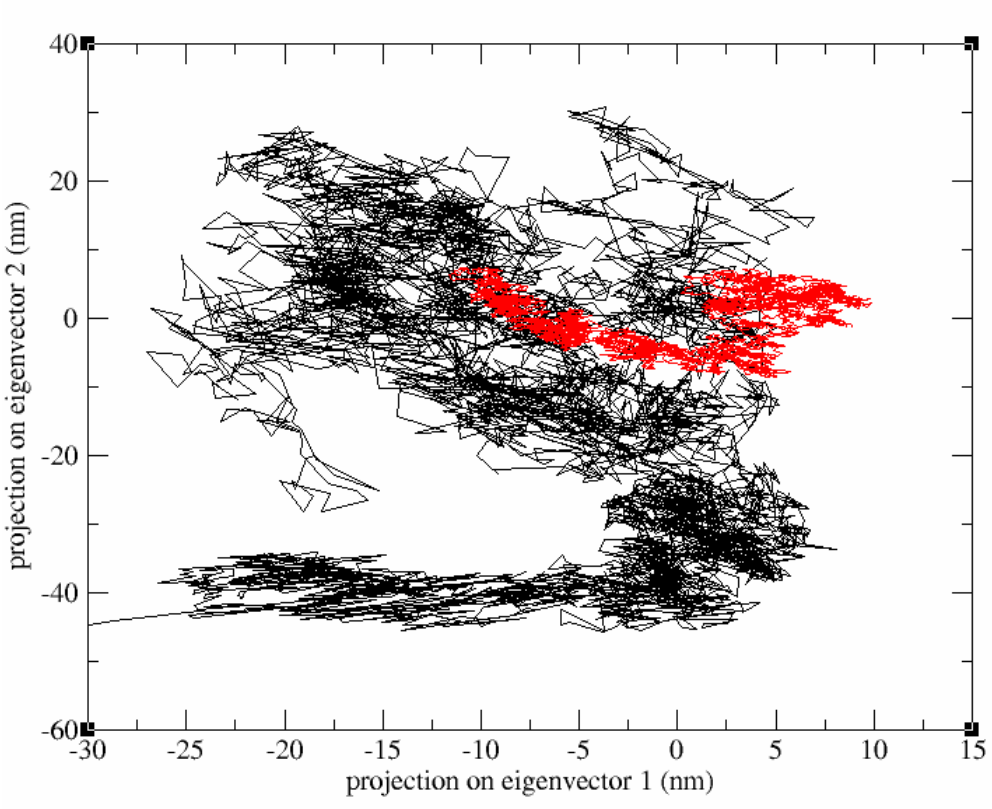

Fig. 7 Projection of most significant principal components of motion of the Cα- atoms of PBP2x. The trajectory projected to the two-dimensional space. Black color indicates PBP2x in the absence of Ceftobiprole, PBP2x-Ceftobiprole complex shown in red.

Table 1 Crystal structure of Penicillin binding proteins and β-lactamase selected for this study

S.No	PDB ID	Detail	Source	Reference
1	1VQQ	Structure of Penicillin binding protein 2A (chain B)	*Staphylococcus aureus.*	Lim and Strynadka, 2002
2	2WAE	Penicillin binding protein 2B (Chain A)	*Streptococcus pneumoniae*	Martel et al., 2009
3	1PYY	Penicillin binding protein 2X (chain B)	*Streptococcus pneumoniae*	Yamada et al., 2007
4	1IYS	Crystal structure of class A β-lactamase toho-1 (chain A)	*Escherichia coli*	Ibuka et al., 2003

Table 2 Docking results of β-lactam antibiotics with Penicillin binding proteins (PBP2A, PBP2B & PBP2X) and SHV-1 β-lactamase

S.No	Ligands	PBP2a (Dock score)	PBP2b (Dock score)	PBP2x (Dock score)	Shv-1 β-lactamase (Dock score)
1	Cefepime	3.3	3.1	3.9	5.9
2	Cefozopran	4.2	3.3	1.7	4.9
3	Cefpirome	3.4	4.1	3.2	5.6
4	Cefquinome	3.2	4.2	4.0	4.5
5	Ceftaroline	4.0	3.9	3.6	5.9
6	Ceftobiprole	5.2	5.6	6.0	3.2
7	Doripenem	4.2	4.0	3.8	6.8
8	Ertapenem	4.3	5.1	4.2	4.3
9	Faropenem	3.7	4.8	2.1	5.0
10	Imipenem	3.9	3.9	3.5	4.2
11	Meropenem	4.8	3.8	3.8	5.5
12	Tebipenem	4.2	2.8	4.5	5.6
13	Thienamycin	4.3	4.5	3.5	6.1

Table.3 Post docking results for β-lactam antibiotics with PBP2a

S. No.	ligand- Enzyme complex	Interacting residues	No. of H-bonds
1	Cefepime -pbp2a	His293, Asp295, Glu239	3
2	Cefozopran- pbp2a	His293, Asp295, Lys148	3
3	Cefpirome- pbp2a	Lys273	1
4	Cefquinome- pbp2a	Asp295	1
5	Ceftaroline- pbp2a	Tyr297	2
6	Ceftobiprole- pbp2a	Gln292, Asp295, His293	5
7	Doripenem- pbp2a	His293, Asp295, Glu239	5
8	Ertapenem- pbp2a	Asp295, Ser149, Lys148, Thr165	4
9	Faropenem- pbp2a	Ser149, Lys48	2
10	Imipenem- pbp2a	Asp295, Val277, Gln292	5
11	Meropenem- pbp2a	Asp295, Lys148,Glu239	5
12	Tebipenem- pbp2a	His293, Asn146	2
13	Thienamycin- pbp2a	Lys273, Val277, His293	3

Table. 4 Post docking results for β-lactam antibiotics with PBP2b

S. No.	Ligand-Enzyme complex	Interacting residues	No. of H-bonds
1	Cefepime -pbp2b	Asp222, Glu240, Lys77	3
2	Cefozopran- pbp2b	Lys77, Lys241, Glu240, Arg262, Ser238, Arg223	6
3	Cefpirome- pbp2b	Ile225,Arg223, Arg262, Lys77	6
4	Cefquinome- pbp2b	Lys77, Asp222, Glu240, Ser239	4
5	Ceftaroline- pbp2b	Ser231, Ile225, Arg223	3
6	Ceftobiprole- pbp2b	Lys241, Arg223, Ser239, Glu240, Ser238, Arg262	7
7	Doripenem- pbp2b	Arg223, Glu246, Lys77, Thr194	6
8	Ertapenem- pbp2b	Trp221, Val237, Gly243	3
9	Faropenem- pbp2b	Arg223, Asp222, Lys77, Glu240	6
10	Imipenem- pbp2b	Lys241, Glu240, Lys77	4
11	Meropenem- pbp2b	Glu240, Arg262, Val237, Ser236	4
12	Tebipenem- pbp2b	Ser235, Thr265, Lys270, Thr267	4
13	Thienamycin- pbp2b	Arg223, Asp222, Lys77, Arg262, Lys241	5

Table. 5 Post docking results for β-lactam antibiotics with PBP2x

S. No.	Ligand- Enzyme complex	Interacting residues	No. of H-bonds
1	Cefepime -pbp2x	Arg186, Asn185, Ser93, Asn95, Asp313	6
2	Cefozopran- pbp2x	Asp313, Asn185, Ser93	3
3	Cefpirome- pbp2x	Thr92, Lys75	2
4	Cefquinome- pbp2x	Thr159, Gly157, Tyr129	3
5	Ceftaroline- pbp2x	Lys75, Thr78, Tyr80, Glu89	4
6	Ceftobiprole- pbp2x	Asp313,Asp90, Thr92, Ser93	7
7	Doripenem- pbp2x	Thr92	1
8	Ertapenem- pbp2x	Glu89, Lys75, Asp257	3
9	Faropenem- pbp2x	Glu89, Thr78, Asp90, Lys75	4
10	Imipenem- pbp2x	Asp131, Tyr129, Thr159, Asn156	4
11	Meropenem- pbp2x	Ala91, Asn95	2
12	Tebipenem- pbp2x	Thr78, Glu89	2
13	Thienamycin- pbp2x	Lys154, Leu130, Tyr129, Asn162	4

Table.6 Post docking results for β-lactam antibiotics with SHV-1 β-lactamase

S. No.	Ligand-enzyme complex	Interacting residues	No. of H-bonds
1	Cefepime -SHV-1	Asn104, Arg274, Asp240	6
2	Cefozopran- SHV-1	Thr216, Arg276, Gly236, Ser130	4
3	Cefpirome- SHV-1	Asn132, Arg276, Arg274, Asp240	6
4	Cefquinome- SHV-1	Arg276, Arg274, Glu273, Tyr105	5
5	Ceftaroline- SHV-1	Asn104, Thr216, Arg276, Ser237, Arg274	7
6	Ceftobiprole- SHV-1	Arg276, Gln270, Asn132	3
7	Doripenem- SHV-1	Asn132, Ser237, Ser130, Thr216, Arg276	8
8	Ertapenem- SHV-1	Thr215, Ser130, Lys234, Ser70, Ser237	5
9	Faropenem- SHV-1	Ser130, Ser70, Asn132	6
10	Imipenem- SHV-1	Arg274, Ser237, Asn132	4
11	Meropenem- SHV-1	Asn104, Arg274, Ser137, Arg276	7
12	Tebipenem- SHV-1	Ser237, Arg276, Ser130, Tyr105	7
13	Thienamycin- SHV-1	Ser130, Asn132, Glu166, Asn170, Ser70, Ser137, Arg274	8

Table 7 Dock score, H-bond interactions and bond length obtained for Ceftobiprole with PBP2a, PBP2b, PBP2x and SHV-1

Protein-ligand complex	Dock score	H-bond interaction	Bond length (Å)	Bond Angle (°)
PBP2a-Ceftobiprole	5.2	(Gln292)OE1-H55	2.1	147
		(Asp295)OD1-H41	2.2	142
		(His293)O-H54	1.8	131
		(His293)O-N26	3.3	160
		(Asp295)OD2-N28	2.8	145
PBP2b-Ceftobiprole	5.6	(Lys241)N2-O34	2.5	144
		(Arg223)O-H55	2.0	138
		(Ser239)OG-O17	2.5	165
		(Ser239)OG-H53	2.5	171
		(Glu240)N-O20	3.2	158
		(Ser238)O-O29	2.9	148
		(Arg262)NH1-O20	3.3	143
PBP2x-Ceftobiprole	6.0	(Asp313OD1-H41	2.1	156
		(Asp313)OD2-H41	2.2	171
		(Asp90)O-H58	2.7	146
		(Ala91)O-O17	2.9	166
		(Thr92)O-O17	2.8	136
		(Thr92)O-O20	3.2	162
		(Ser93)HG-O33	2.8	145
SHV-1-Ceftobiprole	3.2	(Arg276)NH2-O17	2.9	140
		(Gln270)O-H41	2.0	138
		(Asn132)ND2-O29	3.0	155